

Design, Synthesis, and Biological Evaluation of *N*-Carboxyphenylpyrrole Derivatives as Potent HIV Fusion Inhibitors Targeting gp41

Kun Liu,[†] Hong Lu,[‡] Ling Hou,[†] Zhi Qi,[‡] Cátia Teixeira,[§] Florent Barbault,[§] Bo-Tao Fan,[§] Shuwen Liu,^{||} Shibo Jiang,^{*,‡,||} and Lan Xie^{*,†}

Beijing Institute of Pharmacology & Toxicology, 27 Tai-Ping Road, Beijing, 100850, China, Lindsley F. Kimball Research Institute, New York Blood Center, New York, New York 10065, ITODYS, University Paris 7—CNRS UMR 7086, 1 rue Guy de la Brosse, 75005 Paris, France, School of Pharmaceutical Sciences, Southern Medical University, Guangzhou, 510515, China

Received July 14, 2008

On the basis of the structures of small-molecule hits targeting the HIV-1 gp41, *N*-(4-carboxy-3-hydroxy)phenyl-2,5-dimethylpyrrole (**2**, NB-2), and *N*-(3-carboxy-4-chloro)phenylpyrrole (**A**₁, NB-64), 42 *N*-carboxyphenylpyrrole derivatives in two categories (A and B series) were designed and synthesized. We found that 11 compounds exhibited promising anti-HIV-1 activity at micromolar level and their antiviral activity was correlated with their inhibitory activity on gp41 six-helix bundle formation, suggesting that these compounds block HIV fusion and entry by disrupting gp41 core formation. The structure–activity relationship and molecular docking analysis revealed that the carboxyl group could interact with either Arg579 or Lys574 to form salt bridges and two methyl groups on the pyrrole ring were favorable for interaction with the residues in gp41 pocket. The most active compound, *N*-(3-carboxy-4-hydroxy)phenyl-2,5-dimethylpyrrole (**A**₁₂), partially occupied the deep hydrophobic pocket, suggesting that enlarging the molecular size of **A**₁₂ could improve its binding affinity and anti-HIV-1 activity for further development as a small-molecule HIV fusion and entry inhibitor.

Introduction

According to the estimate of UNAIDS, about 33.2 million people worldwide are living with HIV and more than 25 million patients have died of AIDS (www.unaids.org/en/Knowledge-Centre/HIVData/EpiUpdate/EpiUpdArchive/2007/). Thus far, 28 anti-HIV drugs have been licensed by the United States Food and Drug Administration (FDA) (http://www.hivandhepatitis.com/hiv_and_aids/hiv_treat.html). Most of these drugs belong to two categories: reverse transcriptase inhibitors (RTI) and protease inhibitors (PI). Combined application of these antiretroviral drugs has shown significant synergistic effects.¹ However, an increasing number of patients with HIV infection/AIDS can no longer use such drugs as a result of drug resistance and serious adverse effects.^{2–4} Therefore, it is essential to develop novel anti-HIV drugs targeting HIV entry.

HIV-1 envelope glycoprotein (Env) transmembrane subunit gp41 plays an important role in virus fusion and entry⁵ and can serve as a target for the development of HIV-1 fusion inhibitors.^{6,7} The gp41 ectodomain contains a fusion peptide (FP), the N- and C-terminal heptad repeat (NHR and CHR, respectively). The peptides derived from the gp41 CHR region (designated C-peptides) are potent HIV fusion inhibitors.^{8–10} One of the C-peptides, T-20 (**1**, Enfuvirtide, a 36-amino acid synthetic peptide)^{11,12} was approved by the US FDA in 2003 as the first member of a new class of anti-HIV drugs—HIV fusion inhibitors for treating HIV/AIDS patients who have failed to respond to RTI and PI. Drug **1** was believed to interact with the HIV-1 gp41 NHR and block the gp41 six-helix bundle (6-

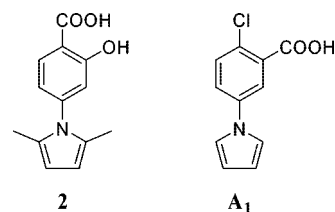


Figure 1. Structures of hits **2** and **A**₁.

HB) core formation, thereby inhibiting fusion between the viral and target cell membranes.^{10,13,14} Although **1** is very potent in inhibiting HIV infection, it has two critical limitations as a drug: lack of oral availability and high production cost.¹⁵ Therefore, it is necessary to develop orally available nonpeptide small-molecule fusion inhibitors but with a mechanism of action similar to C-peptides. By screening a drug-like chemical library using a high-throughput screening technique,¹⁶ we previously identified two small molecules, *N*-(4-carboxy-3-hydroxy)phenyl-2,5-dimethylpyrrole (**2**, NB-2) and *N*-(3-carboxy-4-chloro)phenylpyrrole (**A**₁, NB-64)¹⁷ (Figure 1), which inhibit HIV-1 fusion and entry by interfering with the gp41 6-HB formation. These promising hits prompted us to focus on the modification of **2** and **A**₁ to discover and develop new lead compounds with novel scaffold and higher potency. Here we report the results of our hit-to-lead process, including design, synthesis, and biological evaluation of 42 *N*-carboxyphenyl pyrroles and related derivatives. Their primary structure–activity relationships are discussed.

Design. Previous studies have identified an attractive target in gp41 for small-molecule HIV fusion inhibitors, i.e., the deep hydrophobic pocket (~16 Å long, ~7 Å wide, and 5–6 Å deep) on the surface of the internal N-helix trimer that is filled by three conserved hydrophobic residues with large side chains (Ile635, Trp631, and Trp628) in the gp41 CHR region.^{13,18} The combined molecular mass of these residues inside the pocket is ~600 Da, which is within the size range for binding of an

* To whom correspondence should be addressed. L. Xie and S. Jiang, For L.X.: phone, 86-10-6818-1014; Fax, 86-10-6821-1656, E-mail: lanxieshi@yahoo.com. For S. J.: phone, 212-570-3058; fax, 212-570-3099; E-mail: SJiang@NYBloodCenter.org.

[†] Beijing Institute of Pharmacology & Toxicology.

[‡] Lindsley F. Kimball Research Institute, New York Blood Center.

[§] ITODYS, University Paris 7—CNRS UMR 7086.

^{||} School of Pharmaceutical Sciences, Southern Medical University.

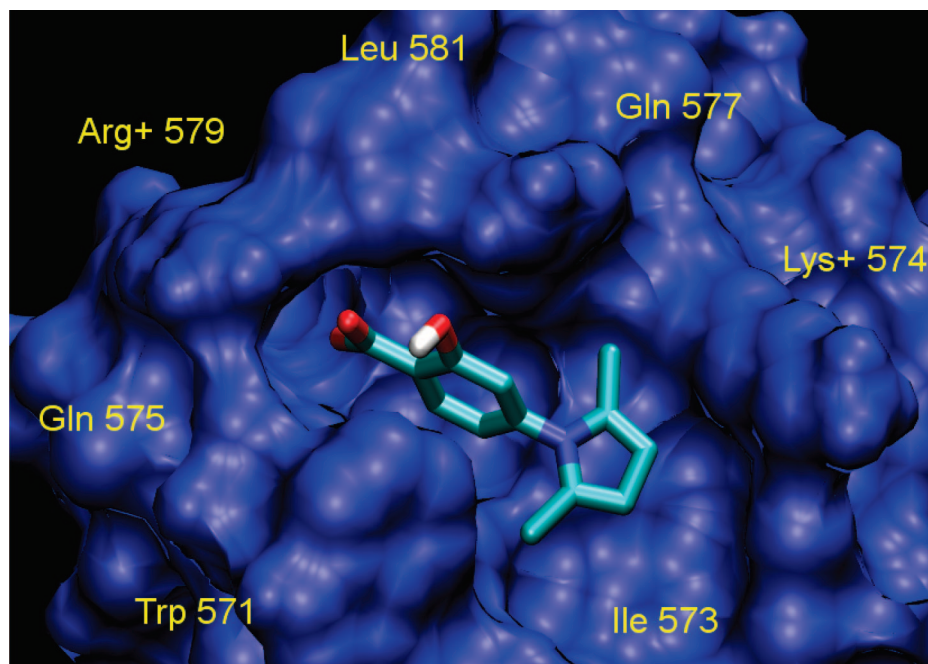


Figure 2. Molecular modeling: the docking conformation of **2** inside the hydrophobic pocket of gp41.

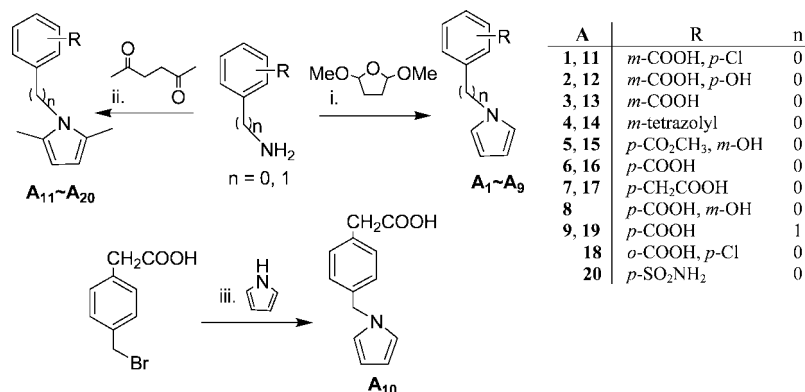
orally bioavailable, small-molecule drug.¹⁹ On the basis of this information, we docked a known hit **2** into the gp41 hydrophobic pocket (Figure 2). This step allowed us to image the gp41 binding “pocket” shape, the orientation and effective binding conformation of inhibitor **2**, and more surface amino acids such as Trp571, Gln575, Arg579, Leu581, Gln577, Lys574, and Ile573. The docking results indicated that **2** partially occupies the pocket. Our previous studies indicated that the carboxyl group of **A**₁ orients to the positively charged Lys574, which is a key surface amino acid in forming a salt “bridge” with an inhibitor.^{20–22} On the other hand, the carboxyl group of **2** interacts with Arg579 rather than Lys574 (Figure 2). Thus, it can be hypothesized that the acid group in the compounds can interact with either of these two positively charged residues around the pocket to form a salt bridge, which stabilizes the interaction between the compound and the HIV-1 gp41. Consequently, our hit-to-lead optimization and rational design aimed at improving the shape complementation with the binding pocket in order to provide more binding points and increase affinity with the biologic target. It is anticipated that these results will, in turn, provide the basis for discovering more potent leads with a new scaffold.

In the hit-to-lead optimization process, both the structural similarities and differences between **2** and **A**₁ led us to explore the structural impact of the phenylpyrrole compounds. Two parallel series of *N*-phenylpyrrole and *N*-phenyl-2,5-dimethylpyrrole derivatives (**A**₁–**A**₁₀ and **A**₁₁–**A**₂₀) with a *p*- or *m*-COOH on the benzene ring were first designed and synthesized to determine which structural moieties are necessary and which position of the carboxyl group is most favorable for anti-HIV potency. Specifically, it was possible that the carboxyl group on the benzene ring could significantly affect the molecular geometry and binding orientation because it is expected to form a salt bridge with Lys574 or Arg579 on the surface of binding site.^{20–22} Next, more boundary substituents were introduced on the *N*-phenylpyrrole skeleton to produce more potential target–inhibitor interaction points for enhancing binding affinity. This resulted in an increase of anti-HIV potency. Meanwhile, an isosteric replacement of the carboxyl group was also performed by a tetrazole moiety. Next, the

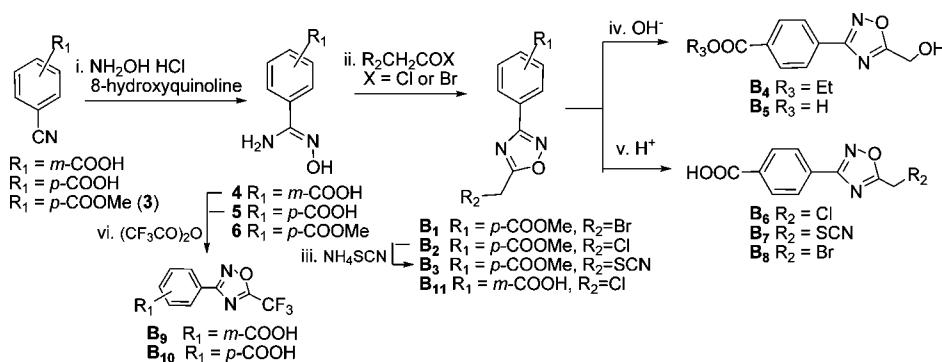
strategy of isosteric replacement was then applied by using several five-membered heterocycles instead of the pyrrole ring to investigate if the pyrrole ring necessary for anti-HIV potency and, hopefully, to identify new potential structural moieties. Therefore, a series of carboxyphenyl compounds with an 1,2,4-oxadiazole (**B**₁–**B**₁₁), thiaziazole (**B**₁₂), maleimide (**B**₁₃–**B**₁₅), or rhodanine (**B**₁₆–**B**₂₂) ring, respectively, were designed and synthesized. In the **B** series of compounds, a polar functional group, or side chain on the five-membered ring could enlarge the size and change the shape of inhibitors. Both the design and modification of all new compounds were driven by bioassays for anti-HIV-1 activity against HIV-1 replication and gp41 six-helix bundle formation. Meanwhile, molecular modeling studies were performed to elucidate the structure and activity relationship for these small-molecule fusion inhibitors.

Chemistry. As shown in Scheme 1, the Paal–Knorr reaction was used to synthesize **A**₁–**A**₉ and **A**₁₁–**A**₂₀ by the condensation of anilines or benzylamines with 2,5-dimethoxytetrahydrofuran or acetylacetone (hexane-2,5-dione),²³ respectively. The Paal–Knorr reaction was performed with or without glacial acetic acid as solvent under microwave irradiation in a sealed tube at 100–150 °C for 10 min.²⁴ Microwave irradiation greatly reduced reaction time and byproducts, resulting in yields ranging from 50 to 88%, which was higher than the 28–56% in the traditional condition. *N*-Benzylpyrrole **A**₁₀ was prepared by treatment of 4-(bromomethyl)phenylacetic acid and pyrrole in the presence of potassium *tert*-butoxide (*t*-BuOK) under microwave irradiation with a yield of 84%. However, the several syntheses to obtain pure **2** as a positive control in our bioassays were unsuccessful even though *N*-(3-carboxy-4-hydroxy)phenyl-2,5-dimethylpyrrole (**A**₁₂), an isomer of **2**, was successfully synthesized with a 79% yield. This appeared to be caused by the instability of **2** during workup and purification when color changed rapidly from white to deep-red.

The 1,2,4-oxadiazole derivatives **B**₁–**B**₁₁ were synthesized by the acylation of amidoxime,²⁴ as shown in Scheme 2. Cyanobenzoic acids or ester were treated with hydroxylamine hydrochloride in the presence of 8-hydroxyquinoline²⁵ to produce corresponding benzamidoximes **4**–**6**, respectively. Compound **6** reacted with either bromoacetyl bromide or

Scheme 1. Synthesis of A₁–A₂₀^a

^a (i) and (ii) AcOH, microwave, 150 °C, 10 min; (iii) *t*-BuOK, DMSO, microwave, 193 °C, 10 min.

Scheme 2. Synthesis of B₁–B₁₁^a

^a (i) Na₂CO₃, EtOH, reflux, 4 h; (ii) THF, reflux, 8 h; (iii) DMF, 90 °C, 3 h; (iv) 1N NaOH, EtOH, rt, 4 h; (v) HCl or HBr/AcOH (1:1), 100 °C, 8–12 h; (vi) pyridine, reflux, 2 h.

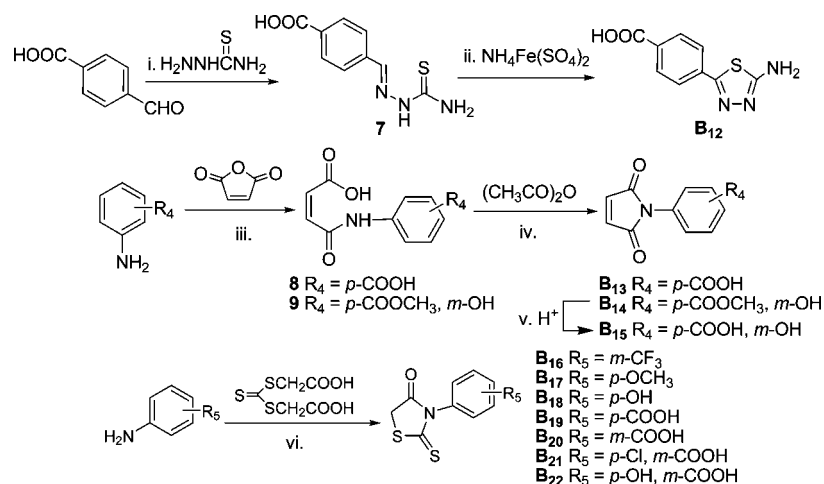
chloroacetyl chloride in THF at reflux temperature to afford 5-substituted 3-aryl-1,2,4-oxadiazoles **B₁** or **B₂**, respectively. 5-Chloromethyl group on the oxadiazole ring of **B₂** was then converted into 5-thiocyanomethyl by treatment with ammonium thiocyanate in DMF at 90 °C to produce **B₃**. Following a basic hydrolysis of **B₁** in EtOH, an ester exchange product 3-(4'-ethoxycarbonyl)phenyl-5-hydroxymethyl oxadiazole (**B₄**) was produced. However, hydrolysis of **B₂** in the basic condition yielded 3-(4'-carboxyl)phenyl-5-hydroxymethyl oxadiazole (**B₅**). Otherwise, esters **B₂** and **B₃** were hydrolyzed in the presence of HCl/AcOH (1:1) to yield corresponding 3-(4'-carboxyl)phenyl-1,2,4-oxadiazoles **B₆** and **B₇**, respectively. The preparation of 5-bromomethyl oxadiazole **B₈** have to hydrolyze **B₁** in HBr/AcOH (1:1), whereas the bromide in **B₁** could be replaced by chloride if the hydrolysis was carried out in HCl/AcOH. By treating with trifluoroacetic anhydride in pyridine, **4** and **5** afforded corresponding 5-trifluoromethyl-1,2,4-oxadiazoles **B₉** and **B₁₀**, respectively. Compound **B₁₁** was synthesized from **4** in one step with a yield of 37%.

The syntheses of **B₁₂–B₂₂** are summarized in Scheme 3. These compounds possess a five-membered heterocyclic ring moiety instead of the pyrrole ring in the A series of compounds. According to methods found in the literature,²⁶ thiosemicarbazone (**7**) was prepared from *p*-carboxylbenzaldehyde by treating with thiosemicarbazide in ethanol followed by a cyclization in aq ammonium ferric sulfate solution to produce 4-carboxyphenyl-1,3,4-thiadiazole (**B₁₂**). Anilines reacted with maleic anhydride afforded intermediate *N*-aryl maleic monoamides **8** and **9**, followed by dehydration and cyclization in acetic anhydride and triethylamine,²⁶ which produced corresponding *N*-aryl maleimide derivatives **B₁₃** and **B₁₄**, respectively. The acidic

hydrolysis of **B₁₄** produced an expected compound **B₁₅**, but a basic hydrolysis destroyed the maleimide ring. Subsequently, *N*-phenyl-substituted rhodanine derivatives **B₁₆–B₂₂** were prepared from various anilines by treatment of bis(carboxymethyl)-trithio carbonate in water with a 28–88% yield, respectively.²⁷ A direct substitution between NH of rhodanine and benzene bromide failed in spite of using various bases, such as potassium *tert*-butoxide, sodium hydride, potassium (or sodium) hydroxide, and potassium carbonate, even though this reaction seemed simple and convenient.

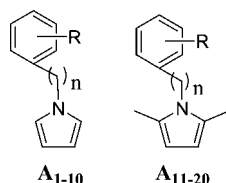
Results and Discussion

A total of 42 newly synthesized *N*-arylpyrrole derivatives (20 in the A series and 22 in the B series) were tested in parallel with **A₁** for their inhibitory activity on HIV-1 replication (as determined by p24 production), HIV-1-mediated cell–cell fusion, and gp41 6-HB formation. The compounds **A₂–A₁₀** and **A₁₁–A₂₀** contain the same backbone structures of **A₁** and **2**, respectively. A majority of these compounds exhibited significant inhibitory activity on HIV-1 replication and gp41 6-HB formation as determined by ELISA and native-PAGE (Table 1 and Figure 3). The anti-HIV-1 activities of these compounds were correlated with their inhibitory activities on 6-HB formation (Figure 4), suggesting that these compounds, like **2** and **A₁**, may interact with the gp41 NHR region to disrupt the fusion-active core formation, resulting in blockage of gp41-mediated membrane fusion and inhibition of HIV-1 replication. Indeed, most of the active compounds displayed inhibitory activity on HIV-1-mediated cell–cell fusion (data not shown). But unlike the majority of the active compounds, a few compounds did not have good correlation between their anti-HIV-1 activity and

Scheme 3. Synthesis of B₁₂–B₂₂^a

^a (i) EtOH, reflux, 1.5 h; (ii) H₂O, reflux, 10 h; (iii) EtOAc, rt, 1 h; (iv) NEt₃, 60 °C, 1 h; (v) HCl/AcOH (1:1), 100 °C, 8 h; (vi) H₂O, 100 °C, 19 h.

Table 1. Anti-HIV Activity Data of Pyrrole Derivatives A₁–A₂₀ as HIV-1 gp-41 Inhibitors



code no.	R on benzene ring				inhibiting p24 production EC ₅₀ (μM)	cytotoxicity CC ₅₀ (μM)	SI ^a	inhibition of 6-HB formation IC ₅₀ (μM)
	<i>p</i> -	<i>m</i> -	<i>o</i> -	<i>n</i> -				
A ₁ (NB-64)	Cl	CO ₂ H	H	0	2.39	335.72	140.47	58.74
A ₂	OH	CO ₂ H	H	0	9.66	492.61	50.99	48.72
A ₃	H	CO ₂ H	H	0	44.81	301.93	6.74	210.7
A ₄	H	tetrazolyl	H	0	41.04	436.11	10.63	226.11
A ₅	CO ₂ CH ₃	OH	H	0	35.44	379.12	10.70	460.83
A ₆	CO ₂ H	H	H	0	69.25	534.76	7.72	129.47
A ₇	CH ₂ CO ₂ H	H	H	0	371.24	497.51	1.34	497.51
A ₈	CO ₂ H	OH	H	0	81.67	442.56	5.42	70.84
A ₉	CO ₂ H	H	H	1	63.93	497.51	7.78	156.72
A ₁₀	CH ₂ CO ₂ H	H	H	1	465.12	465.12		465.12
A ₁₁	Cl	CO ₂ H	H	0	1.52	210.76	138.66	78.68
A ₁₂	OH	CO ₂ H	H	0	0.69	133.46	193.42	37.36
A ₁₃	H	CO ₂ H	H	0	11.81	88.42	7.49	42.23
A ₁₄	H	tetrazolyl	H	0	7.7	249.46	32.40	25.61
A ₁₅	CO ₂ CH ₃	OH	H	0	59.14	88.9	1.50	286.7
A ₁₆	CO ₂ H	H	H	0	173.72	136.28	0.78	188.74
A ₁₇	CH ₂ CO ₂ H	H	H	0	2.1	203.84	97.07	225.15
A ₁₈	Cl	H	CO ₂ H	0	8.56	400.00	46.73	60.34
A ₁₉	CO ₂ H	H	H	1	15.55	298.56	19.20	160.22
A ₂₀	SO ₂ NH ₂	H	H	0	99.08	116.8	1.18	182.44

^a SI = selectivity index, CC₅₀/EC₅₀.

their inhibitory activity on 6-helix bundle formation. One of the explanations is that these active compounds may target more than one step of the HIV life cycle. For example, betulinic acid, a bifunctional anti-HIV-1 compound, inhibits HIV infection by targeting both HIV-1 entry and maturation steps.²⁸ Therefore, it is worthwhile to further investigate the mechanism(s) of action of those compounds that do not have good correlation between their activities against HIV-1 infection and 6-helix bundle formation.

Notably, the 2,5-dimethylpyrrole compounds A₁₁–A₁₄, A₁₇, and A₁₉ were significantly more potent than the corresponding pyrrole compounds A₁–A₄, A₇, and A₉, respectively. This fact, along with previous theoretical work,²⁹ indicated that the two methyl groups on the pyrrole ring and a near perpendicular

conformation between benzene and pyrrole rings by steric crowding effect may be favorable for targeting the gp41 binding site, as shown in Figure 2. Further comparisons between A₁₃ (EC₅₀ 11.81 μM) and A₁₆ (EC₅₀ 173.72 μM), A₂ (EC₅₀ 9.66 μM) and A₈ (EC₅₀ 81.67 μM), and A₃ (EC₅₀ 44.81 μM) and A₆ (EC₅₀ 69.25 μM) indicated that a carboxyl group at the *m*-position of the benzene ring is more suitable than the *p*-position for enhancing anti-HIV potency. After an isosteric replacement of carboxyl, A₁₄ with a tetrazolyl moiety at the *m*-position of the benzene ring was more potent (EC₅₀ 7.70 μM) than A₁₃. More interestingly, compound A₁₄ exhibited more potent inhibitory activity against six-helix bundle formation (IC₅₀ 25.61 μM) than A₁ (IC₅₀ 58.74 μM), suggesting that tetrazolyl moiety could be a potential structural fragment for designing novel small-

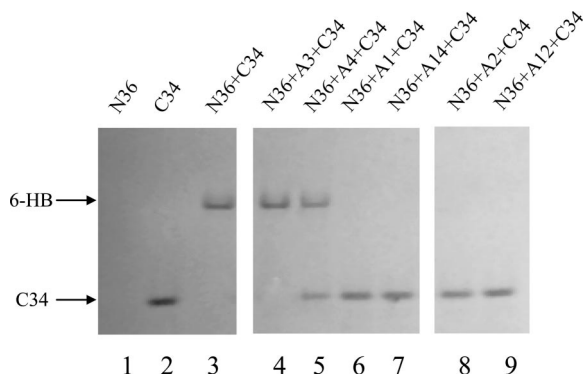


Figure 3. Inhibition of the HIV-1 gp41 6-HB formation by small-molecule compounds (N-PAGE). N36 alone (lane 1) exhibited no band because it carries net positive charges and may migrate off the gel.³⁵ C34 alone (lane 2) displayed a band at a lower position in the gel. The mixture of N36 and C34 (lane 3) showed a band at the upper position in gel, corresponding to that of 6-HB.³⁵ In the presence of **A**₃ (lane 4) and **A**₄ (lane 5), N36 and C34 could still form the 6-HB, while addition of **A**₁ (lane 6), **A**₂ (lane 8), **A**₁₂ (lane 9), and **A**₁₄ (lane 7) resulted in disappearance of the 6-HB band and reappearance of the C34 band, suggesting that these compounds can block the 6-HB formation between N36 and C34.

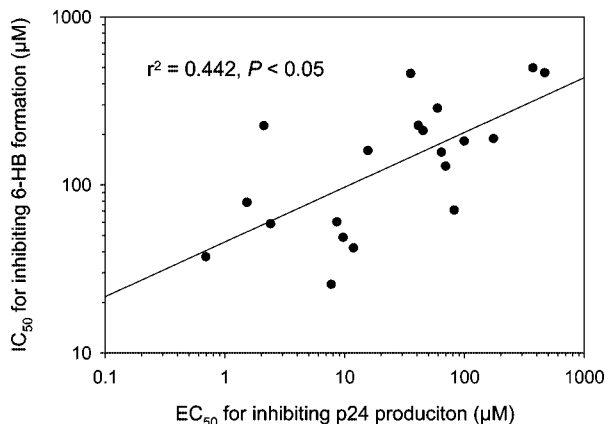


Figure 4. Correlation between the inhibitory activities of the A series compounds on HIV-1 replication and gp41 6-HB formation.

molecule HIV fusion inhibitors targeting gp41. By introducing an additional hydroxyl or chloride on the phenyl ring, compounds **A**₁, **A**₂, **A**₁₁, **A**₁₂, and **A**₁₈ all exhibited potent anti-HIV activity with an EC₅₀ value range of 0.69–9.66 μM. This suggests that more boundary substituents may greatly enhance molecular affinity with the binding site. Meanwhile, compound **A**₁₇, with more linear molecular size exhibited higher potency (EC₅₀ 2.10 μM) than its counterpart **A**₁₆ (EC₅₀ 173.72 μM), thus guiding us to expand molecular size in order to enhance the affinity of inhibitor with the binding site.

Among the phenylpyrrole derivatives, **A**₁₂ was the most effective in inhibiting p24 production (EC₅₀ 0.69 μM) and gp41 6-HB formation (IC₅₀ 37.36 μM). It also effectively inhibited HIV-1-mediated cytopathic effect (CPE) and cell–cell fusion (data not shown). The other two *N*-carboxylphenyl-2,5-dimethylpyrroles, **A**₁₁ and **A**₁₇, also showed promising potency.

To understand and interpret the bioassay results, molecular modeling studies (2D-, 3D-quantitative structure–activity relationship and molecular docking) were performed for the compounds from series A.²⁹ The docking analysis for the two active compounds **A**₁₂ and **A**₁₄ with the hydrophobic pocket of the gp41 N-trimer (Figures 5,6) indicates lower calculated binding free energies of Δ*G*, –6.9 and –5.6 kcal/mol, respec-

tively. The following main interactions between **A**₁₂ and gp41 were expected: (1) interaction of two H-bonds from the hydroxyl group of **A**₁₂ with the main-chain carbonyl oxygen of Gln575 and that of the *m*-carboxyl group of **A**₁₂ with the main-chain amine of Gln577, respectively, (2) an electrostatic interaction between the carboxyl group of **A**₁₂ and Arg579, and (3) hydrophobic interactions of the pyrrole ring with Lys574 and Ile573 and that of the phenyl ring with the Trp571. The electrostatic force oriented **A**₁₂ in the direction of Arg579, and the steric force of the methyl groups of **A**₁₂ resulted in a T-shaped effective binding conformation between the benzene and pyrrole rings. However, **A**₁₄ with a three-aromatic-ring skeleton occupied more binding site space, thus providing more hydrophobic interactions between **A**₁₄ and surface amino acid residues of the gp41 binding site, i.e., the benzene ring with Ile573 and the pyrrole ring with the hydrocarbon chain of Lys574. The tetrazolyl ring with more negative charges orients **A**₁₄ closer to Arg579 and serves as an H donor to form an H-bond with main-chain carbonyl oxygen of Gln572. However, the molecular modeling results indicated that, while both **A**₁₂ and **A**₁₄ have similar binding orientation and perpendicular conformation between aromatic rings, the three-ring angle geometric conformation of **A**₁₄ might match the binding site better, thus enhancing binding affinity.

Among compounds **B**₁–**B**₁₁ with an oxadiazole ring, only a few (e.g., **B**₆ and **B**₁₀) displayed moderate inhibitory activity against HIV-1 replication and 6-HB formation with selectivity index (SI) values >16. However, the B series of compounds with a thiadiazole **B**₁₂, maleimide **B**₁₃–**B**₁₅, or rhodanine ring **B**₁₆–**B**₂₂, respectively, showed no significant inhibitory activity on HIV-1 replication and 6-HB formation (Table 2). The results suggest that these heterocyclic structures may be less effective than pyrrole in interacting with the gp41 pocket and, therefore, less effective in inhibiting HIV-1 fusion and entry.

In conclusion, we have designed and synthesized 42 *N*-carboxyphenylpyrrole derivatives in both the A and B categories. These novel compounds were based on the structures of small-molecule hits targeting the HIV-1 gp41, **2** and **A**₁. We found that a majority of the compounds in the A series exhibited significant inhibitory activity on HIV-1 entry and replication as well as 6-HB formation. Their anti-HIV-1 activity is also correlated with their ability to disrupt the gp41 fusion-active core formation, suggesting that these compounds inhibit HIV-1 fusion and entry in agreement with the mechanism of action of **2** and **A**₁ and the anti-HIV peptide C34.^{15,30} Furthermore, 2,5-dimethylpyrrole compounds were generally more potent than the corresponding pyrrole compounds, suggesting that the presence of dimethyl groups resulted in a favorable T-shape conformation between the benzene and pyrrole rings. Compound **A**₁₂ was the most active compound; therefore, further development is justified. In contrast, the majority of the compounds in the B series showed no significant anti-HIV-1 activity, indicating that these heterocyclic structures might be unfavorable for binding to the gp41 pocket. The docking analysis also suggests that the positively charged residues Arg579 and Lys574 are important for interaction with the compounds by forming salt bridges for stabilizing the binding of the compounds to the hydrophobic pocket. On the other hand, all compounds in the A and B series may not be large enough (<300 Da) to fully occupy the deep hydrophobic pocket, which can accommodate a compound with a mass of ~600 Da. Therefore, current active compounds should be increased in molecular size in order to

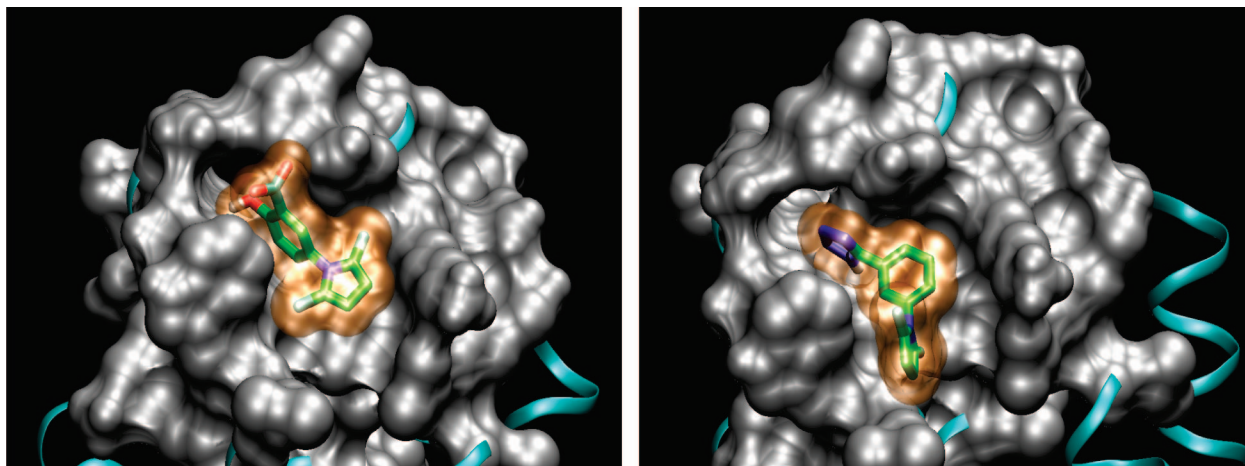


Figure 5. Surface representation of the hydrophobic pocket of HIV-1 gp41 with the docked compound **A**₁₂ (left) or **A**₁₄ (right).

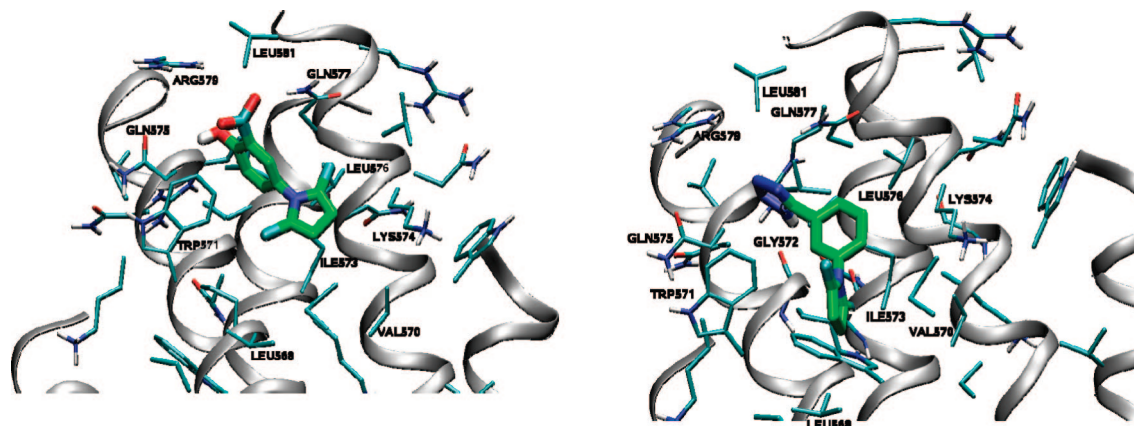


Figure 6. Docking conformations of active compounds **A**₁₂ (left) and **A**₁₄ (right) inside the hydrophobic pocket of HIV-1 gp41 and residues of the pocket surrounding ligands.

improve their efficacy in blocking the 6-HB formation and inhibiting HIV fusion and entry.

Experimental Section

Chemistry. Melting points were measured with a RY-1 melting apparatus without correction. The proton nuclear magnetic resonance (¹H NMR) spectra were measured on a JNM-ECA-400 (400 MHz) spectrometer using tetramethylsilane (TMS) as internal standard. The solvent used was DMSO-*d*₆ unless indicated. Mass spectra (MS) were measured on either a Micromass ZabSpec or an ABI Perkin-Elmer Sciex API-3000 mass spectrometer with electrospray ionization. Elementary analyses were performed with a model-1106 analyzer. Active target compounds were analyzed for C, H, and N and gave values within ±0.4% of the theoretical values. HPLC analyses were performed using an Agilent 1100 series and an Eclipse XDB-C18 column eluting with a mixture of solvents A and B (condition 1: A/B = water/acetonitrile 30:70, flow rate 0.8 mL/min; condition 2: A/B = water/methanol 20:80, flow rate 0.6 mL/min; UV 254 nm). The microwave reactions were performed on a microwave reactor from Biotage, Inc. Thin-layer chromatography (TLC) was performed on silica gel GF₂₅₄ plates. Silica gel GF₂₅₄ (200–300 mesh) from Qingdao Haiyang Chemical Company was used for TLC, preparative TLC, and column chromatography. Medium-pressure column chromatography was performed using a CombiFlash Companion purification system. All chemicals were obtained from Beijing Chemical Works or Sigma-Aldrich, Inc.

General Procedure for the Preparation of *N*-Phenylpyrrole Derivatives **A₁–**A**₇, **A**₉.** To a solution of aminobenzoic acid analogues (1 equiv) in 3 mL of glacial acetic acid was added 2,5-dimethoxy-tetrahydrofuran (1.1 equiv). The mixture was stirred and

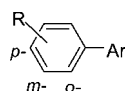
irradiated under microwave at 150 °C for 10 min as monitored by TLC (petroleum ether/EtOAc 3:1). The mixture was poured into ice–water. The solid was filtered out and washed with water and then crude product was purified by flash column (gradual eluant: EtOAc/petroleum ether with AcOH (v/v 1: 0.005) to obtain pure expected product.

***N*-(3-Carboxy-4-chloro)phenylpyrrole (**A**₁, **NB-64**).** Yield: 82%, starting with 331 mg (1.93 mmol) of 5-amino-2-chlorobenzoic acid to afford **A**₁, white solid, mp 125–128 °C. ¹H NMR δ ppm 7.90 (1H, d, *J* = 2.0 Hz, ArH-2), 7.75 (1H, dd, *J* = 8.4 and 2.0 Hz, ArH-6), 7.60 (1H, d, *J* = 8.4 Hz, ArH-5), 7.43 (2H, m, PyH-2,5), 6.29 (2H, t, *J* = 2.2 Hz, PyH-3,4). MS *m/z* (%) 221 (*M*⁺, 100), 223 (*M* + 2, 36). Anal. (C₁₁H₈ClNO₂) C, H, N.

***N*-(3-Carboxy-4-hydroxy)phenylpyrrole (**A**₂).** Yield: 51%, starting with 306 mg (2 mmol) of 5-aminosalicylic acid to afford **A**₂, white solid, mp 178–180 °C. ¹H NMR δ ppm 11.34 (1H, br, COOH), 7.82 (1H, d, *J* = 2.8 Hz, ArH-2), 7.73 (1H, dd, *J* = 9.2 and 2.8 Hz, ArH-6), 7.26 (2H, m, PyH-2,5), 7.07 (1H, d, *J* = 9.2 Hz, ArH-5), 6.24 (2H, t, *J* = 2.2 Hz, PyH-3,4). MS *m/z* (%) 203 (*M*⁺, 100). Anal. (C₁₁H₉NO₃) C, H.

***N*-(3-Carboxy)phenylpyrrole (**A**₃).** Yield: 57%, starting with 274 mg (2 mmol) of 3-aminobenzoic acid to afford **A**₃, white solid, mp 175–178 °C. ¹H NMR δ ppm 13.18 (1H, br, COOH), 7.98 (1H, d, *J* = 2.0 Hz, ArH-2), 7.80 (2H, dd, *J* = 8.4 and 2.0 Hz, ArH-4,6), 7.57 (1H, t, *J* = 8.4 Hz, ArH-5), 7.40 (2H, m, PyH-2,5), 6.26 (2H, t, *J* = 2.2 Hz, PyH-3,4). MS *m/z* (%) 187 (*M*⁺, 100). Anal. (C₁₁H₉NO₂) C, H, N.

***N*-(3-(1*H*-tetrazol-5-yl)phenylpyrrole (**A**₄).** Yield: 88%, starting with 161 mg (1 mmol) of 3-tetrazolyaniline to afford **A**₄, white solid, mp 210–212 °C. ¹H NMR δ ppm 8.19 (1H, d, *J* = 2.0 Hz,

Table 2. Anti-HIV Activity Data of Five-Membered Heterocyclic Compounds **B**₁–**B**₂₂ as HIV-1 gp41 Inhibitors^a

#	R	Aryl		Inhibiting p24 production EC ₅₀ (μM)	Cytotoxicity CC ₅₀ (μM)	SI*	Inhibition of 6-HB formation IC ₅₀ (μM)
		Type	R'				
B ₁	<i>p</i> -COOMe		CH ₂ Br	87.95	32.73	0.37	>336.70
B ₂	<i>p</i> -COOMe		CH ₂ Cl	41.42	14.23	0.34	>395.26
B ₃	<i>p</i> -COOMe		CH ₂ SCN	10.95	43.67	3.99	171.38
B ₄	<i>p</i> -COOEt		CH ₂ OH	373.02	384.84	1.03	177.90
B ₅	<i>p</i> -COOH		CH ₂ OH	152.73	454.55	2.98	26.45
B ₆	<i>p</i> -COOH		CH ₂ Cl	3.91	63.99	16.37	>420.17
B ₇	<i>p</i> -COOH		CH ₂ SCN	67.97	383.14	5.64	177.74
B ₈	<i>p</i> -COOH		CH ₂ Br	127.03	81.91	0.64	>353.36
B ₉	<i>m</i> -COOH		CF ₃	>400	>400	-	>1000
B ₁₀	<i>p</i> -COOH		CF ₃	3.06	82.25	26.88	223.64
B ₁₁	<i>m</i> -COOH		CH ₂ Cl	57.7	64.9	1.12	346.2
B ₁₂	<i>p</i> -COOH			>400	>400	-	>1000
B ₁₃	<i>p</i> -COOH			205.44	>400	>1.95	>1000
B ₁₄	<i>p</i> -COOMe			39.39	66.15	1.68	100.61
	<i>m</i> -OH						
B ₁₅	<i>p</i> -COOH			>400	>400	-	>1000
	<i>m</i> -OH						
B ₁₆	<i>m</i> -CF ₃			115.8	85.4	0.74	>1000
B ₁₇	<i>p</i> -OCH ₃			63.4	89.6	1.41	>1000
B ₁₈	<i>p</i> -OH			35.7	84.9	2.38	>1000
B ₁₉	<i>p</i> -COOH			257.9	143.2	0.56	>1000
B ₂₀	<i>m</i> -COOH			203.7	165.3	0.81	>1000
	<i>m</i> -COOH						
B ₂₁	<i>p</i> -Cl			179.4	155.3	0.87	>1000
	<i>m</i> -COOH						
B ₂₂	<i>m</i> -COOH			165.8	152.0	0.92	>1000
	<i>p</i> -OH						

^a SI* = selectivity index, CC₅₀/EC₅₀.

ArH-2), 7.92 (1H, d, $J = 8.4$ Hz, ArH-4), 7.83 (1H, dd, $J = 8.4$ and 2.0 Hz, ArH-6), 7.71 (1H, t, $J = 8.4$ Hz, ArH-5), 7.47 (2H, m, PyH-2,5), 6.35 (2H, t, $J = 2.2$ Hz, PyH-3,4). MS m/z (%) 211 (M^+ , 100). Anal. ($C_{11}H_9N_5$) C, H, N.

***N*-(3-Hydroxy-4-methoxycarbonyl)phenylpyrrole (A₅)**. Yield: 71%, starting with 167 mg (1 mmol) of methyl 4-aminosalicylate to afford A₅, white solid, mp 121–124 °C. ¹H NMR δ ppm 10.75 (1H, s, OH), 7.85 (1H, d, $J = 8.4$ Hz, ArH-5), 7.52 (2H, m, PyH-2,5), 7.25 (1H, d, $J = 8.4$ Hz, ArH-6), 7.23 (1H, s, ArH-2), 6.31 (2H, t, $J = 2.2$ Hz, PyH-3,4), 3.91 (3H, s, OCH₃). MS m/z (%) 217 (M^+ , 100). Anal. ($C_{12}H_{11}NO_3 \cdot \frac{1}{8}H_2O$) C, H, N.

***N*-(4-Carboxy)phenylpyrrole (A₆)**. Yield: 65%, starting with 274 mg (2 mmol) of 4-aminobenzoic acid to afford A₆, white solid, mp 199–201 °C. ¹H NMR δ ppm 12.92 (1H, br, COOH), 8.01 (2H, d, $J = 8.4$ Hz, ArH-3,5), 7.73 (2H, d, $J = 8.4$ Hz, ArH-2,6), 7.50 (2H, m, PyH-2,5), 6.32 (2H, t, $J = 2.2$ Hz, PyH-3,4). MS m/z (%) 187 (M^+ , 86). Anal. ($C_{11}H_9NO_2$) C, H, N.

***N*-(4-Carboxymethene)phenylpyrrole (A₇)**. Yield: 77%, starting with 151 mg (1 mmol) of 4-aminophenylacetic acid to afford A₇, white solid, mp 161–164 °C. ¹H NMR δ ppm 12.38 (1H, br, COOH), 7.52 (2H, d, $J = 8.4$ Hz, ArH-2,6), 7.34 (2H, m, PyH-2,5), 7.32 (2H, d, $J = 8.4$ Hz, ArH-3,5), 6.26 (2H, t, $J = 2.2$ Hz, PyH-3,4), 3.59 (2H, s, CH₂); MS m/z (%) 201 (M^+ , 64). Anal. ($C_{12}H_{11}NO_2 \cdot \frac{1}{8}H_2O$) C, H, N.

***N*-(4-Carboxy-3-hydroxy)phenylpyrrole (A₈)**. To a solution of A₅ (538 mg, 2.48 mmol) in 10 mL methanol was added 15 mL of 40% aq NaOH, and the mixture was stirred at room temperature for 6 h monitored by TLC (petroleum ether/EtOAc 3:1). The mixture was then poured into water and acidified with 5% aq HCl to pH 3. The solid was collected, washed with water, and purified by flash chromatography [eluant: EtOAc/petroleum ether with AcOH (4:0.02) 0–20%] to afford 157 mg of A₈, 31% yield, white solid, mp 208–210 °C. ¹H NMR δ ppm 13.94 (1H, br, COOH), 10.83 (1H, s, OH), 7.52 (1H, d, $J = 8.4$ Hz, ArH-5), 7.51 (2H, m, PyH-2,5), 7.25 (1H, d, $J = 8.4$ Hz, ArH-6), 7.22 (1H, s, ArH-2), 6.30 (2H, t, $J = 2.2$ Hz, PyH-3,4). MS m/z (%) 203 (M^+ , 100). Anal. ($C_{11}H_9NO_3$) calcd C, H, N.

***N*-(4-Carboxy)benzylpyrrole (A₉)**. Yield: 70%, starting with 151 mg (1 mmol) of 4-aminomethylbenzoic acid to afford A₉, white solid, mp 168–170 °C. ¹H NMR δ ppm 12.92 (1H, br, COOH), 7.90 (2H, d, $J = 8.4$ Hz, ArH-3,5), 7.24 (2H, d, $J = 8.4$ Hz, ArH-2,6), 6.83 (2H, m, PyH-2,5), 6.64 (2H, t, $J = 2.2$ Hz, PyH-3,4), 5.19 (2H, s, CH₂). MS m/z (%) 201 (M^+ , 93). Anal. ($C_{12}H_{11}NO_2$) C, H, N.

***N*-(4-Carboxymethene)benzylpyrrole (A₁₀)**. To a solution of (4-bromomethyl)-phenylacetic acid (57 mg, 0.25 mmol) and pyrrole (0.02 mL, 0.29 mmol) in 2 mL of DMSO was added *t*-BuOK (70 mg, 0.63 mmol). The mixture was stirred and irradiated under microwave at 193 °C for 20 min monitored by TLC (chloroform/methanol/ammonia 6:1:0.1). The mixture was poured into ice–water and acidified with 2N HCl to pH 3. The solid was collected, washed with water, and purified with flash column [eluant: EtOAc/petroleum ether with AcOH (4:0.02), 0–20%] to afford 45 mg of A₁₀, 84% yield, pale-yellow solid, mp 106–109 °C. ¹H NMR δ ppm 12.28 (1H, br, COOH), 7.21 (2H, d, $J = 8.4$ Hz, ArH-3,5), 7.12 (2H, d, $J = 8.4$ Hz, ArH-2,6), 6.80 (2H, m, PyH-2,5), 6.01 (2H, t, $J = 2.2$ Hz, PyH-3,4), 5.06 (2H, s, N-CH₂), 3.53 (2H, s, –CH₂CO); MS m/z (%) 215 (M^+ , 98). Anal. ($C_{13}H_{13}NO_2 \cdot \frac{1}{8}H_2O$) C, H, N.

General Procedure for the Preparation of *N*-Aryl-2,5-dimethylpyrroles A₁₁–A₂₀. To a solution of amino benzoic acid analogues (1 equiv) in 3 mL of glacial acetic acid was added hexane-2,5-dione (1.1 equiv). The reaction mixture was irradiated under microwave at 150 °C for 10 min and monitored by TLC (petroleum ether/EtOAc 3:1). The mixture was poured into ice–water and left overnight. The precipitated solid was filtered, washed with water, and purified by a flash column [gradual eluant: EtOAc/petroleum ether with AcOH (4:0.02), 0–20%] to afford pure expected products.

***N*-(3-Carboxy-4-chloro)phenyl-2,5-dimethylpyrrole (A₁₁)**. Yield: 66%, starting with 343 mg (2 mmol) of 5-amino-2-chlorobenzoic acid to afford A₁₁, white solid, mp 140–142 °C. ¹H NMR δ ppm 13.63 (1H, br, COOH), 7.69 (1H, d, $J = 8.4$ Hz, ArH-5), 7.61 (1H, d, $J = 2.0$ Hz, ArH-2), 7.48 (1H, dd, $J = 8.4$ and 2.0 Hz, ArH-6), 5.83 (2H, s, PyH), 1.98 (6H, s, Py-CH₃ × 2). MS m/z (%) 249 (M^+ , 100), 251 ($M + 2$, 42). Anal. ($C_{13}H_{12}ClNO_2$) C, H, N.

***N*-(3-Carboxy-4-hydroxy)phenyl-2,5-dimethylpyrrole (A₁₂)**. Yield: 79%, starting with 153 mg (1 mmol) of 5-aminosalicylic acid to afford A₁₂, white solid, mp 169–171 °C. ¹H NMR δ ppm 11.50 (1H, br, COOH), 7.54 (1H, d, $J = 2.0$ Hz, ArH-2), 7.43 (1H, dd, $J = 8.4$ and 2.0 Hz, ArH-6), 7.09 (1H, d, $J = 8.4$ Hz, ArH-5), 5.78 (2H, s, PyH), 1.94 (6H, s, Py-CH₃ × 2). MS m/z (%) 231 (M^+ , 100). Anal. ($C_{13}H_{13}NO_3 \cdot \frac{1}{8}H_2O$) C, H, N.

***N*-(3-Carboxy)phenyl-2,5-dimethylpyrrole (A₁₃)**. Yield: 50%, starting with 274 mg (2 mmol) of 3-aminobenzoic acid to afford A₁₃, white solid, mp 145–148 °C. ¹H NMR δ ppm 13.18 (1H, br, COOH), 7.97 (1H, d, $J = 8.4$ Hz, ArH-4), 7.65 (1H, s, ArH-2), 7.62 (1H, t, $J = 8.4$ Hz, ArH-5), 7.52 (1H, d, $J = 8.4$ Hz, ArH-6), 5.78 (2H, s, PyH), 1.92 (6H, s, Py-CH₃ × 2). MS m/z (%) 214 (M^+ , 100). Anal. ($C_{13}H_{13}NO_2$) C, H, N.

***N*-(3-(1H-Tetrazol-5-yl)phenyl-2,5-dimethylpyrrole (A₁₄)**. The mixture of 3-tetrazolylaniline (161 mg, 1 mmol) and hexane-2,5-dione (0.3 mL, 2.5 mmol), without glacial acetic acid, was irradiated under microwave at 100 °C for 10 min to afford 137 mg of A₁₄, 57% yield, white solid, mp 147–148 °C. ¹H NMR δ ppm 8.14 (1H, d, $J = 8.4$ Hz, ArH-4), 7.87 (1H, s, ArH-2), 7.76 (1H, t, $J = 8.4$ Hz, ArH-5), 7.53 (1H, d, $J = 8.4$ Hz, ArH-6), 5.85 (2H, s, PyH), 2.02 (6H, s, Py-CH₃ × 2). MS m/z (%) 239 (M^+ , 76). Anal. ($C_{13}H_{13}N_5$) C, H, N.

***N*-(3-Hydroxy-4-methoxycarbonyl)phenyl-2,5-dimethylpyrrole (A₁₅)**. Yield: 62%, starting with 378 mg (2.26 mmol) of methyl 4-aminosalicylate to afford A₁₅, yellow solid, mp 58–61 °C. ¹H NMR ($CDCl_3$) δ ppm 10.92 (1H, s, OH), 7.94 (1H, d, $J = 8.4$ Hz, ArH-5), 6.86 (1H, d, $J = 2.0$ Hz, ArH-2), 6.76 (1H, dd, $J = 8.4$ and 2.0 Hz, ArH-6), 5.91 (2H, s, PyH), 3.99 (3H, s, OCH₃), 2.08 (6H, s, Py-CH₃ × 2). MS m/z (%) 245 (M^+ , 100); HPLC purity 98.6%.

***N*-(4-Carboxy)phenyl-2,5-dimethylpyrrole (A₁₆)**. Yield: 83%, starting with 274 mg (2 mmol) of 4-aminobenzoic acid to afford A₁₆, white solid, mp 177–179 °C. ¹H NMR δ ppm 13.07 (1H, br, COOH), 8.06 (2H, d, $J = 8.4$ Hz, ArH-3,5), 7.40 (2H, d, $J = 8.4$ Hz, ArH-2,6), 5.83 (2H, s, PyH), 1.99 (6H, s, Py-CH₃ × 2). MS m/z (%) 215 (M^+ , 100). Anal. ($C_{13}H_{13}NO_2$) C, H, N.

***N*-(4-Carboxymethene)phenyl-2,5-dimethylpyrrole (A₁₇)**. Yield 42%, starting with 521 mg (3.45 mmol) of 4-aminophenylacetic acid to afford A₁₇, white solid, mp 110–112 °C. ¹H NMR δ ppm 7.40 (2H, d, $J = 8.4$ Hz, ArH-2,6), 7.20 (2H, d, $J = 8.4$ Hz, ArH-3,5), 5.78 (2H, s, PyH), 3.65 (2H, s, –CH₂), 1.93 (6H, s, Py-CH₃ × 2). MS m/z (%) 229 (M^+ , 100); Anal. ($C_{14}H_{15}NO_2$) C, H, N.

***N*-(4-Chloro-2-carboxy)phenyl-2,5-dimethylpyrrole (A₁₈)**. The mixture of 172 mg (1 mmol) of 2-amino-5-chlorobenzoic acid and 0.3 mL of hexane-2,5-dione (2.5 mmol), without acetic acid, was irradiated under microwave at 100 °C for 10 min to produce 109 mg of A₁₈, 44% yield, pink solid, mp 124–127 °C. ¹H NMR δ ppm 13.16 (1H, br, COOH), 7.86 (1H, d, $J = 2.0$ Hz, ArH-3), 7.75 (1H, dd, $J = 8.4$ and 2.0 Hz, ArH-5), 7.33 (1H, d, $J = 8.4$ Hz, ArH-6), 5.74 (2H, s, PyH), 1.86 (6H, s, Py-CH₃ × 2). MS m/z (%) 248 ($M - H$, 100), 251 ($M + 2$, 47). Anal. ($C_{13}H_{12}ClNO_2 \cdot \frac{1}{8}H_2O$) C, H, N.

***N*-(4-Carboxy)benzyl-2,5-dimethylpyrrole (A₁₉)**. Yield: 77%, starting with 302 mg (2 mmol) of 4-aminomethylbenzoic acid to afford A₁₉, white solid, mp 171–175 °C. ¹H NMR ($CDCl_3$) δ ppm 8.04 (2H, d, $J = 8.4$ Hz, ArH-3,5), 6.98 (2H, d, $J = 8.4$ Hz, ArH-2,6), 5.88 (2H, s, PyH), 5.07 (2H, s, CH₂), 2.13 (6H, s, Py-CH₃ × 2). MS m/z (%) 229 (M^+ , 100). Anal. ($C_{14}H_{15}NO_2$) C, H, N.

***N*-(4-Aminosulfonyl)phenyl-2,5-dimethylpyrrole (A₂₀)**. The mixture of sulfanilamide (172 mg, 1 mmol) and hexane-2,5-dione (0.3 mL, 2.5 mmol), without glacial acetic acid, was irradiated under

microwave at 180 °C for 15 min to afford 188 mg of **A**₂₀, purified with flash chromatography [eluant: EtOAc/petroleum ether with Et₃N (4: 0.02), 0–20%], 75% yield, white solid, mp 158–159 °C. ¹H NMR (CDCl₃) δ ppm 8.05 (2H, d, *J* = 8.4 Hz, ArH-2,6), 7.39 (2H, d, *J* = 8.4 Hz, ArH-3,5), 5.94 (2H, s, PyH), 4.95 (2H, s, –SO₂NH₂), 2.06 (6H, s, Py-CH₃ × 2). MS *m/z* (%) 250 (M⁺, 100). Anal. (C₁₂H₁₄N₂O₂S) C, H, N.

(Z)-(3-Carboxyl)benzamidoxime (4). To a solution of 3-cyanobenzoic acid (588 mg, 4 mmol) in 30 mL ethanol was added hydroxylamine hydrochloric acid (595 mg, 8.56 mmol) in water (3 mL) and sodium carbonate (687 mg, 6.48 mmol) in water (6 mL), successively, in the presence of 8-hydroxyquinoline (2 mg, 0.013 mmol). The mixture was heated to reflux for 4 h monitored by TLC (petroleum ether/EtOAc/AcOH 1:1:0.03). After removal of ethanol solvent under reduced pressure, the residue was diluted with 30 mL water, and the water solution was slowly acidified with 10% HCl to pH 3.2. The white precipitate was filtrated, washed with water to neutral pH, and dried to afford 668 mg of **4**, 93% yield, white solid, mp 197–199 °C. ¹H NMR δ ppm 13.03 (1H, br, COOH), 9.77 (1H, s, OH), 8.27 (1H, s, ArH-2), 7.95 (2H, dd, *J* = 8.4 Hz, ArH-4,6), 7.53 (1H, t, *J* = 8.4 Hz, ArH-5), 5.95 (2H, br, NH₂).

(Z)-(4-Carboxyl)benzamidoxime (5). The preparation was the same as the synthesis of **4**. Starting with 735 mg (5 mmol) of 4-cyanobenzoic acid to afford 611 mg of **5**, 68% yield, white solid, mp 228 °C dec. ¹H NMR δ ppm 13.02 (1H, br, COOH), 9.89 (1H, s, OH), 7.94 (2H, d, *J* = 8.4 Hz, ArH-3,5), 7.80 (2H, d, *J* = 8.4 Hz, ArH-2,6), 5.94 (2H, s, NH₂). MS *m/z* (%) 179 (M – H, 100).

(Z)-(4-Methoxycarbonyl)benzamidoxime (6). The preparation was the same as that of **4**. Starting with methyl 4-cyanobenzoate (**3**) (806 mg, 5 mmol) to afford 901 mg of **6**, white solid, 93% yield, mp 164–166 °C. ¹H NMR δ ppm 9.91 (1H, s, OH), 7.96 (2H, d, *J* = 8.4 Hz, ArH-3,5), 7.83 (2H, d, *J* = 8.4 Hz, ArH-2,6), 5.95 (2H, br, NH₂), 3.86 (3H, s, –OCH₃). MS *m/z* (%) 195 (M + H, 100).

5-Bromomethyl-3-(4-methoxycarbonyl)phenyl-1,2,4-oxadiazole (B₁). The mixture of **6** (388 mg, 2 mmol) and bromoacetyl bromide (0.19 mL, 2.2 mmol) in THF (10 mL) was heated to reflux for 8 h and monitored by TLC (petroleum ether/EtOAc 4:1). After solvent removal, residue was purified by a silica gel column (petroleum ether/EtOAc 4:1) to afford 378 mg of **B**₁, yield 64%, white solid, 100–102 °C. ¹H NMR δ ppm 8.19 (4H, dd, *J* = 8.4 Hz, ArH), 5.03 (2H, s, CH₂), 3.90 (3H, s, –OCH₃). MS *m/z* (%): 296 (M⁺, 48), 298 (M + 2, 44). Anal. (C₁₁H₉BrN₂O₃) C, H, N.

5-Chloromethyl-3-(4-methoxycarbonyl)phenyl-1,2,4-oxadiazole (B₂). Preparation was the same as that described for **B**₁. Chloroacetyl chloride (0.18 mL, 2.2 mmol) was reacted with **6** (388 mg, 2 mmol) to afford **B**₂: 367 mg, 73% yield, white solid, mp 57–58 °C. ¹H NMR δ ppm 8.19 (4H, dd, *J* = 8.4 Hz, ArH), 5.22 (2H, s, CH₂), 3.90 (3H, s, OCH₃). MS *m/z* (%) 252 (M⁺, 37), 254 (M + 2, 13). Anal. (C₁₁H₉ClN₂O₃ · 1/2H₂O) C, H, N.

3-(4-Methoxycarbonyl)phenyl-5-(thiocyanatomethyl)-1,2,4-oxadiazole (B₃). A mixture of **B**₂ (184 mg, 0.73 mmol) and ammonium thiocyanate (228 mg, 3 mmol) in 5 mL of DMF was heated at 90 °C for 3 h and monitored by TLC (petroleum ether/EtOAc 4: 1). The solution was poured into ice–water and a precipitated yellow solid was filtered, washed with water, and purified by a silica gel column (petroleum ether/EtOAc 4:1) to obtain **B**₃: 89 mg, 44% yield, pale-yellow solid, mp 124–126 °C. ¹H NMR δ ppm 8.20 (4H, dd, *J* = 8.4 Hz, ArH), 4.88 (2H, s, CH₂), 3.91 (3H, s, OCH₃). MS *m/z* (%) 275 (M⁺, 46); HPLC purity 98.7%.

3-(4-Ethoxycarbonyl)phenyl-5-hydroxymethyl-1,2,4-oxadiazole (B₄). A solution of **B**₁ (90 mg, 0.3 mmol) in ethanol (3 mL) in the presence of 1 mL of aq NaOH (1N) was stirred at room temperature for 4 h. The mixture was poured into water, acidified with 5% HCl to pH 5, and then extracted with EtOAc three times. Then organic solvent was removed in vacuo, and residue was purified by a silica gel column (petroleum ether/EtOAc 4:1) to afford **B**₄: 52 mg, 70% yield, white solid, mp 145–148 °C. ¹H NMR (CDCl₃) δ ppm 9.05 (1H, s, OH), 8.17 (2H, d, *J* = 8.4 Hz,

ArH-3,5), 7.85 (2H, d, *J* = 8.4 Hz, ArH-2,6), 4.49 (2H, s, –CH₂OH), 4.42 (2H, q, –OCH₂CH₃), 1.44 (3H, t, –CH₂CH₃). ESI-MS *m/z* (%) (C₁₂H₁₂N₂O₄) 248 (M⁺, 100); HPLC purity 97.1%.

3-(4-Carboxy)phenyl-5-hydroxymethyl-1,2,4-oxadiazole (B₅)

A mixture of **B**₂ (30 mg, 0.12 mmol) in ethanol (3 mL) and 1 mL of aq NaOH (1N) was stirred at room temperature for 4 h. After removal of ethanol in vacuo, more water (ca. 8 mL) was added, washed with EtOAc (2 × 5 mL), and acidified with 5% HCl to pH 2. Solid was filtered out, washed with water to neutral pH, and dried to afford **B**₅: 18 mg, 68% yield, white solid, mp 240–242 °C. ¹H NMR δ ppm 13.27 (1H, br, COOH), 11.53 (1H, s, OH), 8.03 (2H, d, *J* = 8.4 Hz, ArH-3,5), 7.88 (2H, d, *J* = 8.4 Hz, ArH-2,6), 4.41 (2H, s, CH₂). MS *m/z* (%) 219 (M-H, 100); HPLC purity 99.6%.

3-(4-Carboxy)phenyl-5-chloromethyl-1,2,4-oxadiazole (B₆)

To a solution of **B**₂ (30 mg, 0.12 mmol) in glacial acetic acid (1 mL) was dropped 1 mL of hydrochloric acid (36–38%). The mixture was heated at 100 °C for 8 h. After cooling to room temperature, precipitated solid was filtered out, washed with water to neutral pH, and dried to afford **B**₆: 16 mg, 55% yield, white solid, mp 210–212 °C. ¹H NMR δ ppm 13.35 (1H, br, COOH), 8.17 (4H, dd, *J* = 8.4 Hz, ArH), 5.22 (2H, s, CH₂). MS *m/z* (%): 237 (M – H, 94), 239 (M – H + 2, 28); HPLC purity 99.2%.

3-(4-Carboxy)phenyl-5-thiocyanatomethyl-1,2,4-oxadiazole (B₇)

Preparation was the same as that described for **B**₆. Starting with 27 mg of **B**₃ to afford **B**₇, 38% yield, white solid, mp 240–244 °C. ¹H NMR δ ppm 13.26 (1H, br, COOH), 8.08 (4H, dd, *J* = 8.4 Hz, ArH), 4.53 (2H, s, CH₂). MS *m/z* (%) 274 (M – CN + K, 100); HPLC purity 96.2%.

5-Bromomethyl-3-(4-carboxy)phenyl-1,2,4-oxadiazole (B₈)

A mixture of **B**₁ (40 mg, 0.13 mmol) in 1 mL of glacial acetic acid and 1 mL hydrobromic acid (40%) was heated at 100 °C for 12 h to afford 25 mg of **B**₈, white solid, 65% yield, mp 209–211 °C. ¹H NMR δ ppm 13.31 (1H, br, COOH), 8.16 (4H, dd, *J* = 8.4 Hz, ArH), 5.02 (2H, s, CH₂). MS *m/z* (%) 283 (M⁺, 69), 281 (M – 2, 100); HPLC purity 99.8%.

3-(3-Carboxyphenyl)-5-(trifluoromethyl)-1,2,4-oxadiazole (B₉)

A mixture of **4** (180 mg, 1 mmol) and trifluoroacetic anhydride (0.42 mL, 3 mmol) in anhydrous pyridine (3 mL) was heated to reflux for 3 h and monitored by TLC (petroleum ether/EtOAc/AcOH 3:1:0.03). The mixture was poured into ice–water and adjusted with HCl (10%) to pH 4, then extracted with EtOAc three times. After solvent was removed, the residue was purified with flash silica column [eluant: EtOAc/petroleum ether with AcOH (4: 0.03) 3–20%] to afford **B**₉: 107 mg, 42% yield, white solid, mp 114–117 °C. ¹H NMR δ ppm 13.48 (1H, s, COOH), 8.58 (1H, s, ArH-2), 8.32 (2H, dd, *J* = 8.4 Hz, ArH-4,6), 7.80 (1H, t, *J* = 8.4 Hz, ArH-5). MS *m/z* (%) 257 (M-H, 65); HPLC purity 97.1%.

3-(4-Carboxyphenyl)-5-(trifluoromethyl)-1,2,4-oxadiazole (B₁₀)

The preparation was the same as that of **B**₉. Starting with **5** (180 mg, 1 mmol) to afford 136 mg of **B**₁₀, white solid, 53% yield, mp 169–171 °C. ¹H NMR δ ppm 13.44 (1H, br, COOH), 8.21 (2H, d, *J* = 8.4 Hz, ArH-3,5), 8.15 (2H, d, *J* = 8.4 Hz, ArH-2,6). MS *m/z* (%) 258 (M⁺, 100); HPLC purity 97.1%.

3-(3-Carboxy)phenyl-5-chloromethyl-1,2,4-oxadiazole (B₁₁)

As described for the preparation of **B**₂, a mixture of **4** (270 mg, 1.5 mmol) and chloroacetyl chloride (0.16 mL, 1.9 mmol) in 8 mL anhydrous THF was refluxed for 4 h. The mixture was poured into ice–water, and precipitated solid was collected, washed with water to neutral pH, and dried in vacuo to afford **B**₁₁: 132 mg, 37% yield, white solid, mp 128–132 °C. ¹H NMR δ ppm 13.39 (1H, s, COOH), 8.56 (1H, s, ArH-2), 8.28 (1H, d, *J* = 8.4 Hz, ArH-4), 8.18 (1H, d, *J* = 8.4 Hz, ArH-6), 7.76 (1H, t, *J* = 8.4 Hz, ArH-5). MS *m/z* (%) 237 (M – H, 62), 239 (M – H + 2, 36); HPLC purity 96.9%.

4-Carboxylbenzaldehyde thiosemicarbazone (7). A solution of 4-carboxybenzaldehyde (450 mg, 3 mmol) and thiosemicarbazide (300 mg, 3.3 mmol) in ethanol (6 mL) was heated to reflux for 1.5 h and monitored by TLC (CHCl₃/CH₃OH/AcOH 3:1:0.05). After reaction mixture was cooled, the solid was filtered out, washed with ethanol, and dried to give 606 mg of **7**, 91% yield, yellow solid,

mp 250 °C dec. ¹H NMR δ ppm 13.04 (1H, br, COOH), 11.56 (1H, s, =CH=), 8.29 (1H, br, NH), 8.11 (2H, br, NH₂), 7.93 (4H, m, ArH). MS *m/z* (%) 222 (M - H, 100).

5-Amino-3-(4-carboxy)phenyl-1,3,4-thiadiazole (B₁₂). Thiocarbonylcarbazone **7** (370 mg, 1.66 mmol) and ammonium ferric sulfate (3.2 g, 6.64 mmol) were soluble in H₂O (15 mL), and the mixture was heated to reflux for 10 h. The mixture was then poured into ice-water, basified with 10% NaOH aq to pH 5, and extracted with EtOAc three times. Next, organic solvent was removed in vacuo, and residue was purified by a silica gel column (CHCl₃/CH₃OH/AcOH 9:1:0.02) to obtain 171 mg of **B₁₂**, 47% yield, yellow solid, mp 240 °C dec. ¹H NMR δ ppm 8.00 (2H, d, *J* = 8.4 Hz, ArH-3,5), 7.84 (2H, d, *J* = 8.4 Hz, ArH-2,6), 7.57 (2H, br, NH₂). MS *m/z* (%) 222 (M + H, 100); HPLC purity 98.9%.

(Z)-4-[(4-Carboxy)phenylamino]-4-oxobut-2-enoic acid (8). A solution of maleic anhydride (108 mg, 1.1 mmol) and 4-aminobenzoic acid (137 mg, 1 mmol) in EtOAc (7 mL) was stirred for 1 h at rt, resulting in production of abundant crystal solid. The solid was filtered and washed with EtOAc to afford 223 mg of **8**, 95% yield, yellow solid, mp 218–220 °C. ¹H NMR δ ppm 12.82 (1H, br, COOH), 10.60 (1H, s, NH), 7.92 (2H, d, *J* = 8.4 Hz, ArH-3,5), 7.74 (2H, d, *J* = 8.4 Hz, ArH-2,6), 6.51 (1H, d, *J* = 12.0 Hz, =CH-2), 6.34 (1H, d, *J* = 12.0 Hz, =CH-3). MS *m/z* (%) 234 (M - H, 100).

(Z)-4-[(3-Hydroxy-4-methoxycarbonyl)phenylamino]-4-oxobut-2-enoic acid (9). The method of synthesis was the same as that of **8**. Starting with 334 mg (2 mmol) of methyl 4-aminosalicylate, 234 mg, 88% yield, yellow solid, mp 204–207 °C. ¹H NMR δ ppm 12.87 (1H, br, COOH), 10.61 (1H, s, OH), 10.56 (1H, s, NH), 7.76 (1H, d, *J* = 8.4 Hz, ArH-5), 7.41 (1H, s, ArH-2), 7.13 (1H, d, *J* = 8.4 Hz, ArH-6), 6.49 (1H, d, *J* = 12.0 Hz, =CH-3), 6.34 (1H, d, *J* = 12.0 Hz, =CH-2), 3.87 (3H, s, OCH₃). MS *m/z* (%) 264 (M - H, 100).

N-(4-Carboxy)phenylmaleimide (B₁₃). A mixture of **8** (223 mg, 0.95 mmol) and triethylamine (0.06 mL, 0.475 mmol) in 3 mL of acetic anhydride was stirred and heated at 60 °C for 1 h. The mixture was poured into ice-water, and the solid isolated by filtration was washed with water to neutral pH and dried in vacuo to afford **B₁₃**: 98 mg, 47% yield, white solid, mp 160–163 °C. ¹H NMR δ ppm 12.91 (1H, br, COOH), 8.05 (2H, d, *J* = 8.4 Hz, ArH-3,5), 7.51 (2H, d, *J* = 8.4 Hz, ArH-2,6), 7.23 (2H, s, maleimide-H). MS *m/z* (%) 217 (M⁺, 100); HPLC purity 98.5%.

N-(3-Hydroxy-4-methoxycarbonyl)phenylmaleimide (B₁₄). Preparation was the same as that of **B₁₃**. Solid **9** (389 mg, 1.47 mmol) was reacted with triethylamine (0.1 mL, 0.73 mmol) in 5 mL of acetic anhydride to afford 132 mg of **B₁₄**, 27% yield, white solid, mp 121–123 °C. ¹H NMR δ ppm 10.62 (1H, s, OH), 7.88 (1H, d, *J* = 8.4 Hz, ArH-5), 7.22 (2H, s, maleimide-H), 7.04 (1H, d, *J* = 2.0 Hz, ArH-2), 7.00 (1H, dd, *J* = 8.4 and 2.0 Hz, ArH-6), 3.90 (3H, s, OCH₃). MS *m/z* (%) 247 (M⁺, 54). Anal. (C₁₂H₉NO₅) C, H, N.

N-(4-Carboxy-3-hydroxy)phenylmaleimide (B₁₅). Compound **B₁₄** (40 mg, 0.16 mmol) was hydrolyzed in the same condition as **B₆** to afford **B₁₅**, yield 79%, white solid, mp 141–144 °C. ¹H NMR δ ppm 12.81 (1H, br, COOH), 11.42 (1H, s, OH), 7.43 (1H, d, *J* = 8.4 Hz, ArH-5), 6.09 (1H, dd, *J* = 8.4 and 2.0 Hz, ArH-6), 6.06 (2H, s, maleimide-H), 5.96 (1H, d, *J* = 2.0 Hz, ArH-2). MS *m/z* (%) 232 (M - H, 11); HPLC purity 97.5%.

General Procedure for the Preparation of N-Phenylrhodanine Derivatives B₁₆–B₂₂. A suspension of aniline analogues (1 equiv) in 4 mL of water was heated to 95 °C until the aniline was fully dissolved. Then bis(carboxymethyl) trithiocarbonate (1.1 equiv) was added. The resulting solution was heated at 100 °C for 19 h and was cooled to room temperature. The precipitated solid was filtrated out and washed with water. The dried solid was purified by silica gel column (petroleum ether/acetone 3:1) or flash silica column [eluant: EtOAc/petroleum ether with HOAc (3:0.03), 20–30%] to obtain pure product.

N-(3-(Trifluoromethyl)phenyl)rhodanine (B₁₆). Yield: 54%, starting with 2 mL (16 mmol) of 3-(trifluoromethyl)aniline to afford **B₁₆**, yellow solid, mp 150–152 °C. ¹H NMR (CDCl₃) δ ppm 7.77

(1H, d, *J* = 8.4 Hz, ArH-4), 7.70 (1H, t, *J* = 8.4 Hz, ArH-5), 7.51 (1H, s, ArH-2), 7.43 (1H, d, *J* = 8.4 Hz, ArH-6), 4.23 (2H, s, CH₂). MS *m/z* (%) 278 (M + H, 17); Anal. (C₁₀H₆F₃NOS₂) C, H, N.

N-(4-Methoxyphenyl)rhodanine (B₁₇). Yield: 87%, starting with 492 mg (4 mmol) of 4-methoxyaniline to afford **B₁₇**, pale-yellow solid, mp 124–127 °C. ¹H NMR (CDCl₃) δ ppm 7.13 (2H, d, *J* = 8.4 Hz, ArH-2,6), 7.05 (2H, d, *J* = 8.4 Hz, ArH-3,5), 4.18 (2H, s, CH₂), 3.85 (3H, s, OCH₃). MS *m/z* (%) 240 (M + H, 14). Anal. (C₁₀H₉NO₂S₂) C, H, N.

N-(4-Hydroxyphenyl)rhodanine (B₁₈). Yield: 88%, starting with 436 mg (4 mmol) of 4-aminophenol to afford **B₁₈**, pale-yellow solid, mp 180–182 °C. ¹H NMR (CDCl₃) δ ppm 9.12 (1H, s, OH), 7.00 (4H, dd, *J* = 8.4 Hz, ArH-2,3,5,6), 4.17 (2H, s, CH₂). MS *m/z* (%) 224 (M - H, 52); HPLC purity 99.6%.

N-(4-Carboxyphenyl)rhodanine (B₁₉). Yield: 77%, starting with 822 mg (6 mmol) of 4-aminobenzoic acid to afford **B₁₉**, pale-white solid, mp 188–190 °C. ¹H NMR δ ppm 13.23 (1H, br, COOH), 8.09 (2H, d, *J* = 8.4 Hz, ArH-3,5), 7.43 (2H, d, *J* = 8.4 Hz, ArH-2,6), 4.40 (2H, s, CH₂). MS *m/z* (%) 252 (M - H, 84); HPLC purity 99.9%.

N-(3-Carboxyphenyl)rhodanine (B₂₀). Yield: 86%, starting with 418 mg (3 mmol) of 3-aminobenzoic acid to afford **B₂₀**, white solid, mp 185–187 °C. ¹H NMR δ ppm 13.27 (1H, br, COOH), 8.05 (1H, d, *J* = 8.4 Hz, ArH-6), 7.87 (1H, s, ArH-2), 7.69 (1H, t, *J* = 8.4 Hz, ArH-5), 7.55 (1H, d, *J* = 8.4 Hz, ArH-4), 4.37 (2H, s, CH₂). MS *m/z* (%) 252 (M - H, 100); HPLC purity 99.8%.

N-(3-Carboxy-4-chlorophenyl)rhodanine (B₂₁). Yield: 81%, starting with 343 mg (2 mmol) of 5-amino-2-chlorobenzoic acid to afford **B₂₁**, white solid, mp 184–186 °C. ¹H NMR δ ppm 13.71 (1H, br, COOH), 7.78 (1H, d, *J* = 2.4 Hz, ArH-6), 7.75 (1H, d, *J* = 8.4 Hz, ArH-3), 7.50 (1H, dd, *J* = 8.4 and 2.4 Hz, ArH-4), 4.35 (2H, s, CH₂). MS *m/z* (%) 286 (M - H, 100), 288 (M - H + 2, 44); HPLC purity 99.5%.

N-(3-Carboxy-4-hydroxyphenyl)rhodanine (B₂₂). Yield: 28%, starting with 306 mg (2 mmol) of 5-aminosalicylic acid to afford **B₂₂**, yellow solid, mp 174–176 °C. ¹H NMR δ ppm: 13.09 (1H, br, COOH), 11.52 (1H, s, OH), 7.72 (1H, d, *J* = 2.4 Hz, ArH-6), 7.41 (1H, dd, *J* = 8.4 and 2.4 Hz, ArH-4), 7.10 (1H, d, *J* = 8.4 Hz, ArH-3), 4.33 (2H, s, CH₂). MS *m/z* (%) 269 (M⁺, 20), 268 (M - H, 100); HPLC purity 99.7%.

Determination of the Inhibitory Activity of the Compounds on HIV-1 Replication. The inhibitory activity of compounds on HIV-1 IIIB replication in MT-2 cells was determined as previously described. In brief, 1 × 10⁴ MT-2 cells were infected with an HIV-1 strain (100 TCID₅₀) in 200 μL of RPMI 1640 medium containing 10% FBS in the presence or absence of a test compound at graded concentrations overnight. Then the culture supernatants were removed and fresh media containing no test compounds were added. On the fourth day postinfection, 100 μL of culture supernatants were collected from each well, mixed with equal volumes of 5% Triton X-100, and assayed for p24 antigen, which was quantitated by ELISA. Briefly, wells of polystyrene plates (Immulon 1B, Dynex Technology, Chantilly, VA) were coated with HIV immunoglobulin (HIVIG), which was prepared from plasma of HIV-seropositive donors with high neutralizing titers against HIV-1_{IIIB}, in 0.085 M carbonate-bicarbonate buffer (pH 9.6) at 4 °C overnight, followed by washes with washing buffer (0.01 M PBS containing 0.05% Tween-20) and blocking with PBS containing 1% dry fat-free milk (Bio-Rad, Inc., Hercules, CA). Virus lysates were added to the wells and incubated at 37 °C for 1 h. After extensive washes, anti-p24 mAb (183-12H-5C), biotin-labeled antimouse IgG1 (Santa Cruz Biotech, Santa Cruz, CA), streptavidin-labeled horseradish peroxidase (Zymed, San Francisco, CA), and the substrate 3,3',5,5'-tetramethylbenzidine (Sigma Chemical Co., St. Louis, MO) were added sequentially. Reactions were terminated by addition of 1N H₂SO₄. Absorbance at 450 nm was recorded in an ELISA reader (Ultra 386, TECAN, Research Triangle Park, NC). Recombinant protein p24 purchased from US Biological (Swampscott, MA) was included for establishing standard dose-response curves. Each sample was tested in triplicate. The percentage of inhibition of p24 production was calculated as previously described.³¹ The effective

concentrations for 50% inhibition (EC₅₀) were calculated using a computer program, designated CalcuSyn,³² kindly provided by Dr. T. C. Chou (Sloan-Kettering Cancer Center, New York, New York).

Assessment of in Vitro Cytotoxicity. The in vitro cytotoxicity of compounds on MT-2 cells was measured by XTT assay.³³ Briefly, 100 μ L of the test compound at graded concentrations were added to equal volumes of cells (5×10^5 /mL) in wells of 96-well plates. After incubation at 37 °C for 4 days, 50 μ L of XTT solution (1 mg/mL) containing 0.02 μ M of phenazine methosulphate (PMS) was added. After 4 h, the absorbance at 450 nm was measured with an ELISA reader. The CC₅₀ (concentration for 50% cytotoxicity) values were calculated using the CalcuSyn program.³²

Sandwich ELISA and Native Polyacrylamide Gel Electrophoresis for Detecting the gp41 6-HB Formation. A sandwich ELISA as previously described³⁴ was used to test the inhibitory activity of the compounds on gp41 six-helix bundle formation. Briefly, peptide N36 (2 μ M) was preincubated with the compound at graded concentrations at 37 °C for 30 min, followed by addition of C34 (2 μ M). In the control experiments, N36 was preincubated with C34 or PBS at 37 °C for 30 min in the absence of the compounds tested. After incubation at 37 °C for 30 min, the mixture was added to wells of a 96-well polystyrene plate which were precoated with IgG (10 μ g/mL) purified from rabbit antisera directed against the gp41 six-helix bundle. Then, the mAb NC-1, biotin-labeled goat-antimouse IgG, SA-HRP, and TMB were added sequentially. Absorbance at 450 nm was read, and the percentage of inhibition by the compounds was calculated as previously described.³⁴ All the samples were tested in triplicate. In addition, a native polyacrylamide gel electrophoresis (N-PAGE)³⁵ was used to confirm the inhibitory activity of the compounds on the gp41 6-HB formation. In brief, the N-peptide N36 (100 μ M) was mixed with an equimolar concentration of the C-peptide C34 in the presence or absence of the compounds tested. The mixtures were incubated at 37 °C for 30 min, followed by the addition of Tris-glycine native sample buffer (Invitrogen, Carlsbad, CA). The samples (20 μ L) were then loaded onto Tris-glycine gels (18%; Invitrogen, Carlsbad, CA), which were run under 125 V constant voltage at room temperature for 2 h. The gels were stained with Coomassie Blue and then visualized with the FluorChem 8800 imaging system (Alpha Innotech Corp., San Leandro, CA).

Acknowledgment. This investigation was supported by grants 2006AA02Z319 and 2006DFA33560 from the Ministry of Science and Technology in China and 2007G06 from Beijing Municipal Science & Technology Commission to L. Xie, grants 2005Z2-E4041 from Guangzhou Science and Technology Key Project and RO1 AI46221 from the U.S. National Institutes of Health to S. Jiang, and the Ph.D. fellowship SFRH/BD/22190/2005 from Fundação para a Ciência e a Tecnologia (Portugal) to Cátia Teixeira.

Supporting Information Available: Elemental analysis and HPLC purity data for final compounds. This material is available free of charge via the Internet at <http://pubs.acs.org>.

References

- De Clercq, E. Antiviral drugs in current clinical use. *J. Clin. Virol.* **2004**, *30*, 115–133.
- Johnson, V. A.; Brun-Vezinet, F.; Clotet, B.; Conway, B.; D'Aquila, R. T.; Demeter, L. M.; Kuritzkes, D. R.; Pillay, D.; Schapiro, J. M.; Telenti, A.; Richman, D. D. Drug resistance mutations in HIV-1. *Top. HIV Med.* **2003**, *11*, 215–221.
- Richman, D. D.; Morton, S. C.; Wrin, T.; Hellmann, N.; Berry, S.; Shapiro, M. F.; Bozzette, S. A. The prevalence of antiretroviral drug resistance in the United States. *AIDS* **2004**, *18*, 1393–1401.
- Carr, A.; Cooper, D. A. Adverse effects of antiretroviral therapy. *Lancet* **2000**, *356*, 1423–1430.
- Moore, J. P.; Jameson, B. A.; Weiss, R. A. and Sattentau, Q. J. 1993. The HIV-cell fusion reaction. In *Viral Fusion Mechanisms*; Bentz, J., Ed.; CRC Press: Boca Raton, FL, 1993; pp 233–289.
- Chan, D. C.; Kim, P. S. HIV entry and its inhibition. *Cell* **1998**, *93*, 681–684.
- Jiang, S.; Zhao, Q.; Debnath, A. K. Peptide and non-peptide HIV fusion inhibitors. *Curr. Pharm. Des.* **2002**, *8*, 563–580.
- Jiang, S.; Lin, K.; Strick, N.; Neurath, A. R. HIV-1 inhibition by a peptide. *Nature* **1993**, *365*, 113.
- Wild, C. T.; Shugars, D. C.; Greenwell, T. K.; McDanal, C. B.; Matthews, T. J. Peptides corresponding to a predictive α -helical domain of human immunodeficiency virus type 1 gp41 are potent inhibitors of virus infection. *Proc. Natl. Acad. Sci. U.S.A.* **1994**, *91*, 9770–9774.
- Lu, M.; Blacklow, S. C.; Kim, P. S. A trimeric structural domain of the HIV-1 transmembrane glycoprotein. *Nat. Struct. Biol.* **1995**, *2*, 1075–1082.
- Kilby, J. M.; Eron, J. J. Novel therapies based on mechanisms of HIV-1 cell entry. *N. Engl. J. Med.* **2003**, *348*, 2228–2238.
- Lalezari, J. P.; Henry, K.; O'Hearn, M.; Montaner, J. S.; Piliero, P. J.; Trottier, B.; Walmsley, S.; Cohen, C.; Kuritzkes, D. R.; Eron, J. J., Jr.; Chung, J.; DeMasi, R.; Donatucci, L.; Drobnies, C.; Delehanty, J.; Salgo, M. Enfuvirtide, an HIV-1 fusion inhibitor, for drug-resistant HIV infection in north and south America. *N. Engl. J. Med.* **2003**, *348*, 2175–2185.
- Chan, D. C.; Fass, D.; Berger, J. M.; Kim, P. S. Core structure of gp41 from the HIV envelope glycoprotein. *Cell* **1997**, *89*, 263–273.
- Weissenhorn, W.; Dessen, A.; Harrison, S. C.; Skehel, J. J.; Wiley, D. C. Atomic Structure of the Ectodomain from HIV-1 gp41. *Nature* **1997**, *387*, 426–428.
- Liu, S.; Wu, S.; Jiang, S. HIV entry inhibitors targeting gp41: from polypeptides to small-molecule compounds. *Curr. Pharm. Des.* **2007**, *13*, 143–162.
- Liu, S.; Boyer-Chatenet, L.; Lu, H.; Jiang, S. Rapid and automated fluorescence-linked immunosorbent assay for high throughput screening of HIV-1 fusion inhibitors targeting gp41. *J. Biomol. Screening* **2003**, *8*, 685–693.
- Jiang, S.; Lu, H.; Liu, S.; Zhao, Q.; He, Y.; Debnath, A. K. N-substituted pyrrole derivatives as novel human immunodeficiency virus type 1 entry inhibitors that interfere with the gp41 six-helix bundle formation and block virus fusion. *Antimicrob. Agents Chemother.* **2004**, *48*, 4349–4359.
- Chan, D. C.; Chutkowski, C. T.; Kim, P. S. Evidence that a prominent cavity in the coiled coil of HIV type 1 gp41 is an attractive drug target. *Proc. Natl. Acad. Sci. U.S.A.* **1998**, *95*, 15613–15617.
- Malashkevich, V. N.; Chan, D. C.; Chutkowski, C. T.; Kim, P. S. Crystal structure of the simian immunodeficiency virus (SIV) gp41 core: Conserved helical interactions underlie the broad inhibitory activity of gp41 peptides. *Proc. Natl. Acad. Sci. U.S.A.* **1998**, *95*, 9134–9139.
- Jiang, S.; Debnath, A. K. A salt bridge between an N-terminal coiled coil of gp41 and an antiviral agent targeted to the gp41 core is important for anti-HIV-1 activity. *Biochem. Biophys. Res. Commun.* **2000**, *270*, 153–157.
- He, Y.; Liu, S.; Jing, W.; Lu, H.; Cai, D.; Chin, D. J.; Debnath, A. K.; Kirchoff, F.; Jiang, S. Conserved residue Lys574 in the cavity of HIV-1 gp41 coiled-coil domain is critical for six-helix bundle stability and virus entry. *J. Biol. Chem.* **2007**, *282*, 25631–25639.
- He, Y.; Liu, S.; Li, J.; Lu, H.; Qi, Z.; Liu, Z.; Debnath, A. K.; Jiang, S. Conserved salt-bridge between the N- and C-terminal heptad repeat regions of HIV-1 gp41 core structure is critical for virus entry and inhibition. *J. Virol.* **2008**, *82*, 11129–11139.
- Chiu, P. K.; Sammes, M. P. The synthesis and chemistry of azolenines. Part 18. Preparation of 3-ethoxycarbonyl-3h-pyrroles via the Paal-Knorr reaction, and sigmatropic rearrangements involving competitive ester migrations to *c*-2, *c*-4 and *n*. *Tetrahedron* **1990**, *46*, 3439–3456.
- Santilli, A. A.; Morris, R. L. Synthesis of 3-arylsulfonylmethyl-1,2,4-oxadiazole-5-carboxylic acid derivatives. *J. Heterocycl. Chem.* **1979**, *16*, 1197–1200.
- Cottrell, D. M.; Capers, J.; Salem, M. M.; DeLuca-Fradley, K.; Croft, S. L.; Werbovetz, K. A. Antikinetoplastid activity of 3-aryl-5-thiocyanatomethyl-1,2,4-oxadiazoles. *Bioorg. Med. Chem.* **2004**, *12*, 2815–2824.
- Yu, C. Y.; Li, C. X.; Wang, C.; Wang, Z. H. Preparation and performance evaluation of maleimide type bactericides. *Ind. Water Treat.* **2004**, *24*, 36–41.
- Powers, J. P.; Piper, D. E.; Li, Y.; Mayorga, V.; Anzola, J.; Chen, J. M.; Jaen, J. C.; Lee, G.; Liu, J.; Peterson, M. G.; Tonn, G. R.; Ye, Q.; Walker, N. P.; Wang, Z. SAR and mode of action of novel non-nucleoside inhibitors of hepatitis C NS5b RNA polymerase. *J. Med. Chem.* **2006**, *49*, 1034–1046.
- Huang, L.; Yuan, X.; Aiken, C.; Chen, C. H. Bifunctional anti-human immunodeficiency virus type 1 small molecules with two novel mechanisms of action. *Antimicrob. Agents Chemother.* **2004**, *48*, 663–665.

- (29) Teixeira, C.; Barbault, F.; Rebehmed, J.; Liu, K.; Xie, L.; Lu, H.; Jiang, S.; Fan, B.; Maurel, F. Molecular modeling studies of N-substituted pyrrole derivatives—potential HIV-1 gp41 inhibitors. *Bioorg. Med. Chem.* **2008**, *16*, 3039–3048.
- (30) Liu, S.; Lu, H.; Xu, Y.; Wu, S.; Jiang, S. Different from the HIV fusion inhibitor C34, the anti-HIV drug Fuzeon (T-20) inhibits HIV-1 entry by targeting multiple sites in gp41 and gp120. *J. Biol. Chem.* **2005**, *280*, 11259–11273.
- (31) Zhao, Q.; Ma, L.; Jiang, S.; Lu, H.; Liu, S.; He, Y.; Strick, N.; Neamati, N.; Debnath, A. K. Identification of *N*-phenyl-*N'*-(2,2,6,6-tetramethylpiperidin-4-yl)-oxalamides as a new class of HIV-1 entry inhibitors that prevent gp120 binding to CD4. *Virology* **2005**, *339*, 213–225.
- (32) Chou, T. C.; Hayball, M. P. *CalcuSyn: Windows Software for Dose Effect Analysis*; BIOSOFT: Ferguson, MO 63135, 1991.
- (33) Debnath, A. K.; Radigan, L.; Jiang, S. Structure-based identification of small molecule antiviral compounds targeted to the gp41 core structure of the human immunodeficiency virus type 1. *J. Med. Chem.* **1999**, *42*, 3203–3209.
- (34) Jiang, S.; Lin, K.; Zhang, L.; Debnath, A. K. A screening assay for antiviral compounds targeted to the HIV-1 gp41 core structure using a conformation-specific monoclonal antibody. *J. Virol. Methods* **1999**, *80*, 85–96.
- (35) Liu, S.; Zhao, Q.; Jiang, S. Determination of the HIV-1 gp41 postfusion conformation modeled by synthetic peptides: applicable for identification of the HIV-1 fusion inhibitors. *Peptide* **2003**, *24*, 1303–1313.

JM800869T